Cell, Vol. 123, 105–118, October 7, 2005, Copyright ©2005 by Elsevier Inc. DOI 10.1016/j.cell.2005.07.033

Common Molecular Pathways Mediate Long-Term Potentiation of Synaptic Excitation and Slow Synaptic Inhibition

Cindy Shen Huang,[1,2,5] Song-Hai Shi,[1,5] Jernej Ule,[4] Matteo Ruggiu,[4] Laura A. Barker,[3] Robert B. Darnell,[4] Yuh Nung Jan,[1] and Lily Yeh Jan[1,*]
[1]Howard Hughes Medical Institute and
Departments of Physiology and Biochemistry
[2]Graduate Program in Oral and Craniofacial Sciences
[3]Graduate Program in Neuroscience
University of California, San Francisco
San Francisco, California 94143
[4]Howard Hughes Medical Institute and
Laboratory of Molecular Neuro-Oncology
The Rockefeller University
New York, New York 10021

Summary

Synaptic plasticity, the cellular correlate for learning and memory, involves signaling cascades in the dendritic spine. Extensive studies have shown that long-term potentiation (LTP) of the excitatory postsynaptic current (EPSC) through glutamate receptors is induced by activation of N-methyl-D-asparate receptor (NMDA-R)—the coincidence detector—and Ca^{2+}/calmodulin-dependent protein kinase II (CaMKII). Here we report that the same signaling pathway in the postsynaptic CA1 pyramidal neuron also causes LTP of the slow inhibitory postsynaptic current (sIPSC) mediated by metabotropic $GABA_B$ receptors ($GABA_B$-Rs) and G protein-activated inwardly rectifying K^+ (GIRK) channels, both residing in dendritic spines as well as shafts. Indicative of intriguing differences in the regulatory mechanisms for excitatory and inhibitory synaptic plasticity, LTP of sIPSC but not EPSC was abolished in mice lacking Nova-2, a neuronal-specific RNA binding protein that is an autoimmune target in paraneoplastic opsoclonus myoclonus ataxia (POMA) patients with latent cancer, reduced inhibitory control of movements, and dementia.

Introduction

Signaling between neurons involves not only ionotropic receptors, ligand-gated ion channels that generate fast synaptic potentials, but also metabotropic receptors—G protein-coupled receptors with prolonged effects (Hille, 1992). The spines, small protrusions from dendrites, harbor the great majority of excitatory synapses and both types of glutamate receptors (Harris, 1999; Sheng and Kim, 2002), whereas dendritic shafts provide the setting for most inhibitory synapses involving γ-aminobutyric acid (GABA), the major inhibitory transmitter in the mammalian brain (Somogyi et al., 1998). Intrigued by the finding that metabotropic $GABA_B$ receptors ($GABA_B$-Rs) and G protein-activated inwardly rectifying K^+ (GIRK) channels reside on not only dendritic shafts but also the spines (Drake et al., 1997; Kulik et al., 2003), we wondered whether the slow synaptic inhibition mediated by $GABA_B$-Rs and GIRK channels (Lüscher et al., 1997; Marshall et al., 1999) is affected by the machinery in the spine for inducing synaptic plasticity of the glutamate-receptor-mediated excitatory postsynaptic current (EPSC) (Harris, 1999; Malinow, 2003; Nicoll, 2003; Sheng and Kim, 2002).

Intensive studies over decades have identified N-methyl-D-asparate receptor (NMDA-R) as the coincidence detector that allows the postsynaptic neuron to respond to synchronous excitatory inputs with long-lasting changes of synaptic excitation mediated by α-amino-3-hydroxy-5-methyl-4-isoxazole propionic acid receptors (AMPA-Rs) (Bliss and Collingridge, 1993). Optimal NMDA-R activation requires glutamate binding concurrent with postsynaptic depolarization to relieve channel block by external Mg^{2+} ions, so as to allow Ca^{2+} and other cations to go through, thereby activating downstream second messengers such as Ca^{2+}/calmodulin-dependent protein kinase II (CaMKII) and altering synaptic efficacy (Daw et al., 1993). It is an open question whether the signaling cascade mobilized by activation of NMDA-Rs also has long-lasting effects on the slow inhibitory postsynaptic current (sIPSC) mediated by $GABA_B$-Rs and GIRK channels that localize in dendritic spines of glutamatergic neurons, such as CA1 pyramidal neurons, and could be activated via "spillover" of GABA released from inhibitory nerve terminals.

In this study, we found that coincidence detection of synaptic release of glutamate and CA1 pyramidal-neuron depolarization caused long-term potentiation (LTP) of sIPSC, a process dependent on postsynaptic NMDA-R activation, Ca^{2+} increase, and CaMKII activity. To further explore the functional requirement for this novel form of synaptic plasticity, we examined the role of the RNA binding protein Nova-2, an autoimmune target likely important for cognitive functions (Albert and Darnell, 2004; Yang et al., 1998).

Paraneoplastic opsoclonus myoclonus ataxia (POMA) patients, often with latent breast cancer, fallopian cancer, or small cell lung cancer, display ataxic movements and cognitive loss, probably due to the autoimmune responses developed against neuronal-specific antigens expressed by their cancer cells (Buckanovich et al., 1993; Hormigo et al., 1994; Luque et al., 1991; Pranzatelli, 1992). The proteins recognized by their autoimmune antibodies, Nova-1 and Nova-2, are RNA binding proteins that control alternative splicing of multiple gene products for the establishment and function of the central neuronal circuitry (Jensen et al., 2000; Ule et al., 2005). Interestingly, many of the targets of Nova-1 and Nova-2 contribute to inhibitory synaptic transmission and/or synaptic plasticity. Whereas Nova-1 acts primarily in the spinal cord, Nova-2 is expressed mostly in the brain and associates with the RNAs coding for $GABA_B$-Rs and GIRK channels (Jensen et al., 2000; Ule et al., 2003; Yang et al., 1998), essential molecular mediators of sIPSC.

Interestingly, while the Nova-2 null mice exhibited

*Correspondence: gkw@itsa.ucsf.edu
[5]These authors contributed equally to this work.

basal sIPSC comparable to that in control sibling mice, they failed to show LTP of sIPSC, indicating that one of the physiological functions of Nova-2 is to enable activity-dependent modulation of the strength of slow synaptic inhibition. Because the Nova-2 null mice still exhibited LTP of EPSC, Nova-2 appears to be specifically involved in the NMDA-R-mediated synaptic plasticity of slow synaptic inhibition.

Results

GIRK2 Also Resides in the Dendritic Spines of Hippocampal Neurons

GABA causes slow synaptic inhibition by stimulating $GABA_B$-Rs so as to release $G_{\beta\gamma}$ subunits for GIRK-channel activation (Lüscher et al., 1997). Whereas $GABA_B$-Rs are obligate dimers of the R1 and R2 subunits (Marshall et al., 1999), GIRK channels in most central neurons are heterotetramers containing GIRK1 and GIRK2 subunits (Liao et al., 1996; Wickman et al., 2000; Yamada et al., 1998). We therefore began our study by testing whether GIRK2, like $GABA_B$-Rs and GIRK1 (Drake et al., 1997; Kulik et al., 2003), also resides in spines. Indeed, in cultured rat hippocampal neurons expressing the enhanced green fluorescence protein (EGFP) to highlight the spines, strong GIRK2 immunofluorescence was found in the spines (Figure 1A), which house excitatory synapses and harbor the signaling cascade for the LTP of EPSC (Figure 1B) (Harris, 1999; Lisman et al., 2002; Sheng and Kim, 2002).

The sIPSC Mediated by $GABA_B$-Rs and GIRK Channels in CA1 Pyramidal Neurons

To ask whether activation of NMDA-R in the spines causes long-lasting changes of sIPSC, we used rat hippocampal organotypic slice culture, a well-established preparation for studying LTP of the EPSC (Hayashi et al., 2000; Stein et al., 2003), and used the pairing protocol for optimal NMDA-R activation (Hayashi et al., 2000; Kauer et al., 1988). Because CA1 pyramidal neurons and their distal apical dendrites, which possess many GIRK1-containing spines (Drake et al., 1997), tend to receive inhibitory synaptic inputs from interneurons that straddle the border of stratum radiatum (s.r.) and stratum lacunosum-moleculare (s.l.m.) (Vida et al., 1998), we placed the stimulation electrode 300–500 μm from stratum pyramidale (s.p.)—likely within s.l.m. By giving test stimuli at a low frequency to sample the sIPSC before and after the pairing, we asked whether NMDA-R activation via the pairing protocol could alter the sIPSC.

We recorded sIPSC from CA1 pyramidal neurons with whole-cell patch-clamp in the presence of antagonists for AMPA-Rs (5 μM NBQX) and $GABA_A$-Rs (100 μM picrotoxin) and used relatively large nerve stimulation to elicit detectable sIPSC with a single stimulus. With the resultant activation of a large number of glutamatergic nerve fibers, the basal NMDA-R activation (Collingridge et al., 1988) yielded a detectable inward current (NMDA-R EPSC) while neurons were held at −60 mV (Figure 1C), though optimal NMDA-R activation still required depolarization to between −20 mV and 0 mV (see Figure S1 in the Supplemental Data available with this article online). The NMDA-R EPSC (peak latency, 31 ± 9 msec) was followed with a slow outward current (peak latency, 320 ± 81 msec)—the sIPSC, which was blocked by two structurally unrelated GIRK-channel blockers, SCH23390 (10 μM, n = 6) (Kuzhikandathil and Oxford, 2002) (Figure 1C) and tertiapin (100 nM, n = 4) (Bichet et al., 2004) (Figure 1D), and the $GABA_B$-R antagonist SCH50911 (25 μM, n = 7) (Bolser et al., 1995) (Figure 1E). There was relatively little correlation between the amplitudes of NMDA-R EPSC and sIPSC (linear correlation coefficient $R^2 = 0.5$), both of which remained stable when sampled at 0.33 Hz (sIPSC, 93% ± 10% at ~20 min, n = 9, p = 0.3; NMDA-R EPSC, 110% ± 4% at ~20 min, n = 9, p = 0.6) (Figure 2A).

The Pairing Protocol Causes Long-Lasting Potentiation of the sIPSC

Pairing 3 Hz stimulation with depolarization (between −5 mV and 0 mV) for ~2.5 min caused potentiation of sIPSC recorded at −60 mV with 0.33 Hz stimulation. This sIPSC potentiation was robust and long lasting; the sIPSC amplitude increased by ~4-fold (415% ± 40% at ~20 min after pairing, n = 12, p < 0.001), and the potentiation persisted for ~30 min—throughout the duration of the experiment (Figure 2B)—without any changes of the input resistance or the series resistance (Figure 2C) or any significant pairing-induced changes of the NMDA-R EPSC peak amplitude (136% ± 50% at ~20 min after pairing, n = 12, p = 0.2) (Figure 2B) or decay time (measured in the presence of SCH50911, NBQX, and picrotoxin to isolate the NMDA-R EPSC; 97 ± 17 msec before pairing, n = 7; 90 ± 10 msec after pairing, n = 10, p = 0.7) (Figure 2D). Moreover, by measuring the area of sIPSC instead of the peak amplitude, we still observed a persistent and robust pairing-induced potentiation (normalized area, 2.9 ± 0.5 at ~20 min after pairing, n = 12, p < 0.05) (Figure 2E). There was also no clear correlation between the extent of the sIPSC potentiation and the baseline amplitude of sIPSC (linear correlation $R^2 = 0.4$) (Figure 2F) or NMDA-R EPSC ($R^2 = 0.1$) (Figure 2G). Finally, whereas the potentiated sIPSC after pairing was sensitive to the $GABA_B$-R antagonist SCH50911 (n = 4; Figure 3A) and the GIRK-channel blocker SCH23390 (n = 3; Figure 3B), the $GABA_B$-R activity was not required during pairing for the sIPSC potentiation (257% ± 35% at ~30 min after pairing, n = 8, p < 0.005; Figure 3C). Thus, pairing synaptic glutamate release with CA1 pyramidal-neuron depolarization resulted in LTP of sIPSC.

We then asked whether the pairing protocol could also cause potentiation of sIPSC in CA1 pyramidal neurons of acute hippocampal slices from 25- to 30-day-old rats. Because interneurons in the distal apical dendritic field of CA1 pyramidal neurons have a high target preference for not only dendritic shafts but also spines (Vida et al., 1998) and the spines in s.l.m. are particularly rich in GIRK1 immunoreactivity (Drake et al., 1997), we selectively delivered stimuli to the perforant path at s.l.m. The baseline sIPSC sampled with 0.33 Hz stimulation exhibited modest rundown; the sIPSC amplitude ~20 min after initiation of whole-cell patch-clamp recording was 80% ± 27% of the starting value (n = 13, p = 0.02) (Figure 3D). Nonetheless, the pairing protocol

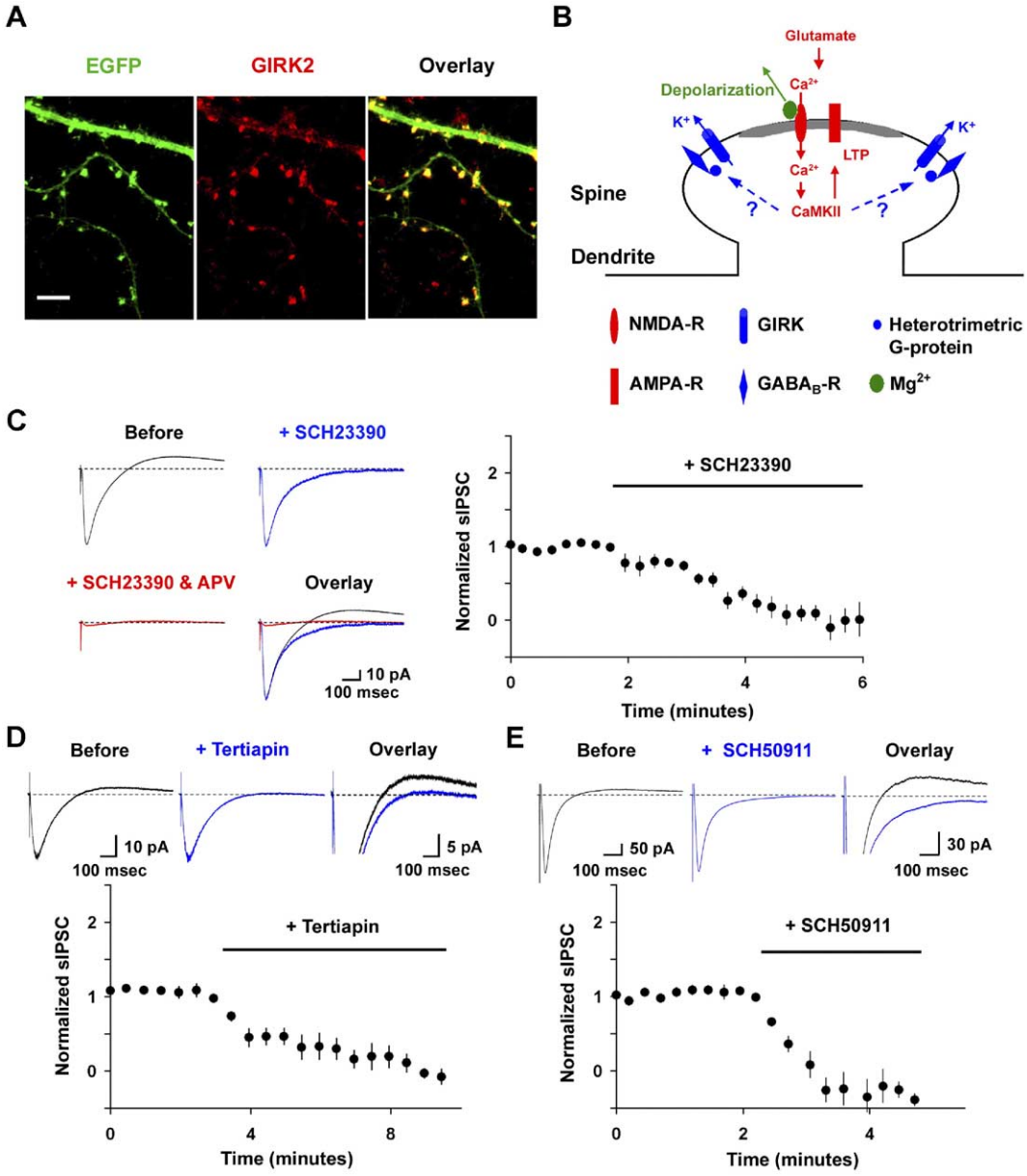

Figure 1. Slow Synaptic Inhibition Mediated by $GABA_B$-Rs and GIRK Channels

In this and all other figures, error bars indicate the standard errors of the mean; no error bars are shown when the standard errors are smaller than the symbol used.

(A) Prominent GIRK2 immunofluorescence (red) in dendritic spines of EGFP-expressing neurons (green). Scale bar: 10 μm.

(B) Signaling cascades in the spine for inducing LTP of EPSC. Glutamate concurrent with depolarization relieving the Mg^{2+} blockade causes optimal NMDA-R activation, Ca^{2+} entry, and CaMKII activation.

(C) GIRK-channel blocker SCH23390 reduced the biphasic response (black) to the NMDA-R EPSC (blue) that is sensitive to APV (red) (n = 6). The time course of sIPSC reduction is also shown.

(D) Another GIRK-channel blocker, tertiapin, also eliminated the sIPSC (n = 4).

(E) The sIPSC is sensitive to the $GABA_B$-R antagonist SCH50911 (n = 7). The overlay of the last two panels is shown at different scale to highlight the sIPSC.

induced persistent potentiation of sIPSC (142% ± 13% at ~20 min after pairing, n = 14, $p < 0.01$) (Figure 3E). Perhaps because of the relatively large stimulation strength necessary for a single stimulus to elicit detectable sIPSCs in the acute slice, the pairing protocol caused some potentiation of NMDA-R EPSC, similar to what has been reported previously (Aniksztejn and Ben-Ari, 1995; Bashir et al., 1991; Watt et al., 2004). Thus, pairing postsynaptic depolarization with perforant-path stimulation was effective in inducing synaptic plasticity in the acute slice. Moreover, without concurrent postsynaptic depolarization, the 3 Hz stimulation

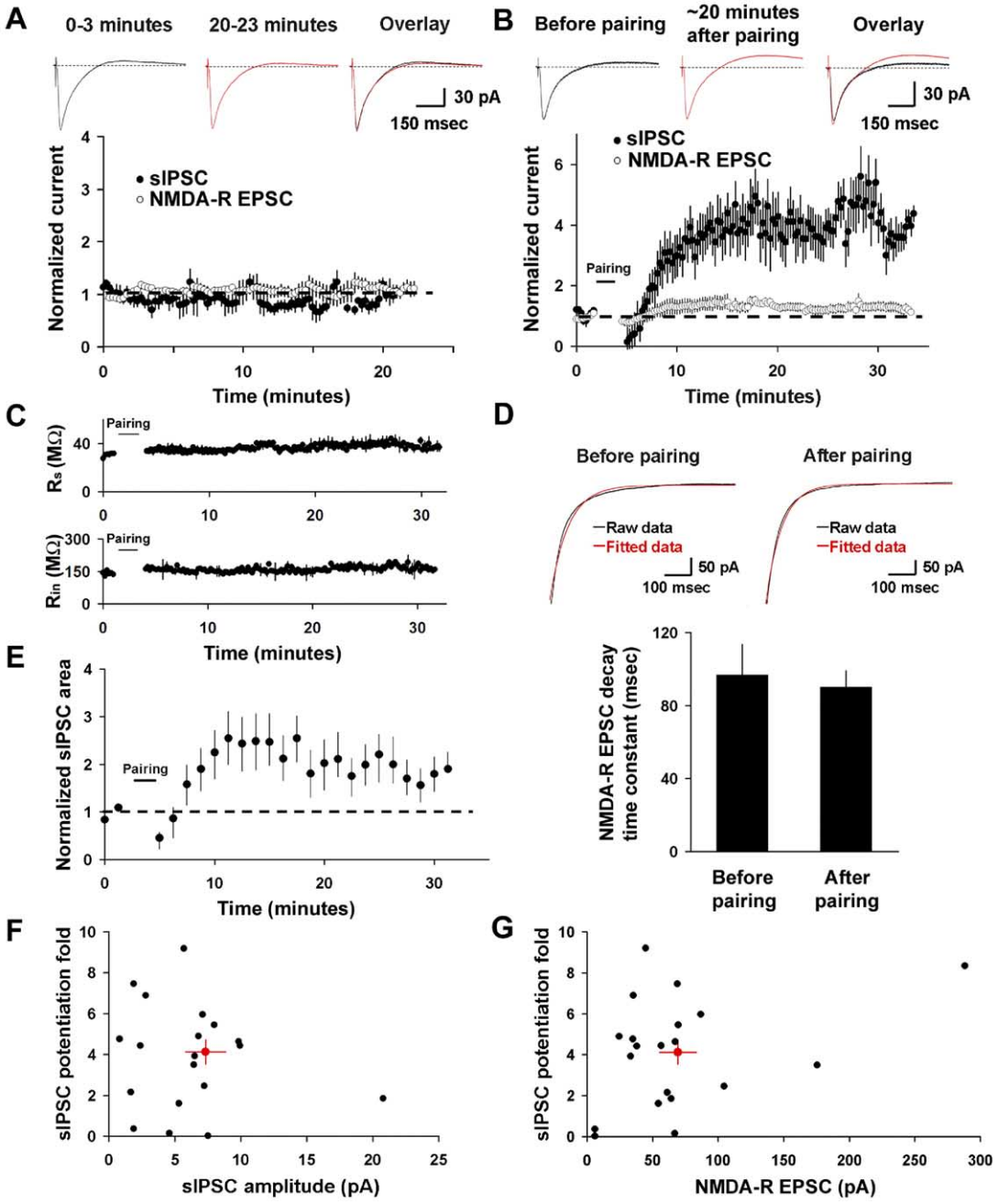

Figure 2. Pairing-Induced LTP of sIPSC in Hippocampal CA1 Pyramidal Neurons

(A) Hippocampal slice culture with fairly stable baseline of sIPSC (filled circles, n = 9, p = 0.3) and NMDAR-EPSC (open circles, n = 9, p = 0.6) sampled at 0.33 Hz. Example traces (average of ~40–60 episodes) are shown above plots of peak amplitudes in this and subsequent figures.

(B) Pairing 3 Hz stimulation with depolarization (–5 to 0 mV) for ~2.5 min potentiated the sIPSC (filled circles, n = 12, p < 0.001) but not NMDA-R EPSC (open circles, n = 12, p = 0.2).

(C) The series resistance R_s (top) and the input resistance R_{in} (bottom) remained constant after pairing (n = 12).

(D) The NMDA-R EPSC decay time constant (n = 7), measured in the presence of SCH50911, NBQX, and picrotoxin, was not altered after pairing (n = 10, p = 0.7) (bottom). Sample traces (black) are compared with idealized traces generated with the average decay time constant (red) (top).

(E) Pairing-induced LTP of the sIPSC as assessed by integrating the sIPSC amplitude over time (n = 12, p < 0.05).

(F) No correlation between the amplitude and the extent of sIPSC potentiation (linear correlation index $R^2 = 0.4$). The average is shown in red in this and the subsequent panel.

(G) No correlation between the extent of sIPSC potentiation and the NMDA-R EPSC amplitude ($R^2 = 0.1$).

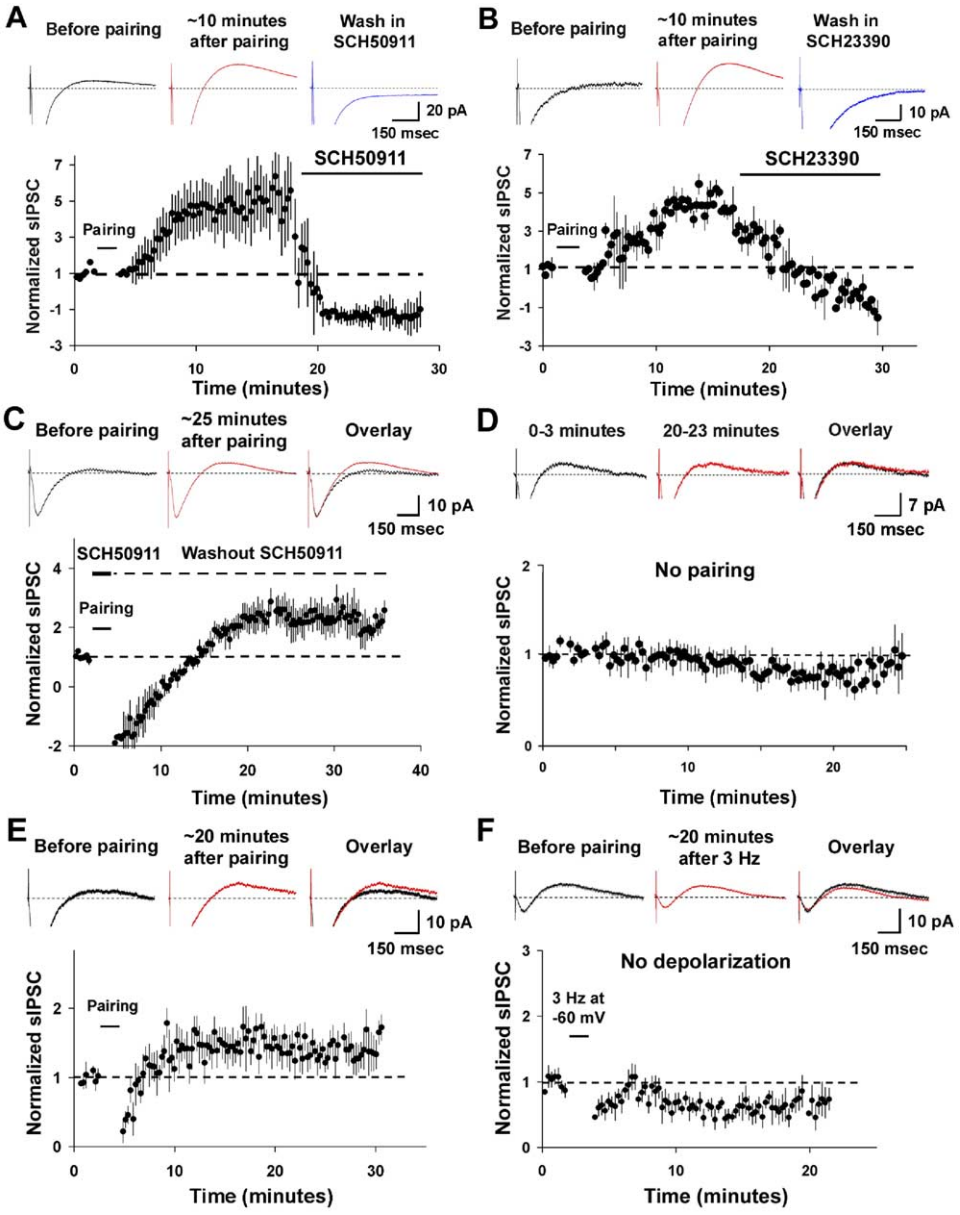

Figure 3. Pairing-Induced sIPSC Potentiation in Slice Cultures and Acute Slices

(A) The potentiated sIPSC in slice culture was sensitive to the $GABA_B$-R antagonist SCH50911 (n = 4).

(B) The potentiated sIPSC was sensitive to the GIRK-channel blocker SCH23390 (n = 3).

(C) Blocking the $GABA_B$-Rs with SCH50911 during pairing did not prevent the induction of sIPSC LTP in slice culture (n = 8, $p < 0.005$).

(D) Acute hippocampal slice exhibited modest rundown of the sIPSC (n = 13, p = 0.02) elicited with perforant-path stimulation.

(E) Pairing-induced potentiation of sIPSC elicited with perforant-path stimulation (n = 14, $p < 0.01$) in acute slices.

(F) Perforant-path stimulation at 3 Hz without concurrent depolarization caused no potentiation of sIPSC in acute slices (n = 8, $p < 0.01$).

failed to potentiate the sIPSC (65% ± 14% at ~20 min after pairing, n = 8, $p < 0.01$; Figure 3F), suggesting that pairing-induced NMDA-R activation is necessary for sIPSC LTP.

Potentiation of the sIPSC Requires NMDA-R Activation in the Postsynaptic CA1 Pyramidal Neuron

To test whether NMDA-R activity is necessary for pairing-induced sIPSC potentiation in slice culture, we first applied the NMDA-R antagonist APV (100 μM) and found no pairing-induced LTP of the sIPSC (102% ± 20% at ~20 min after pairing, n = 7, p = 0.1) (Figure 4A). However, not only was the inward current very small in the presence of antagonists for both NMDA-R and AMPA-R, the sIPSC amplitude was greatly reduced, likely due to inefficient synaptic excitation of the inhibitory interneurons to generate disynaptic sIPSC. We therefore conducted two additional controls. First, we stimulated presynaptic fibers at 3 Hz without depolariz-

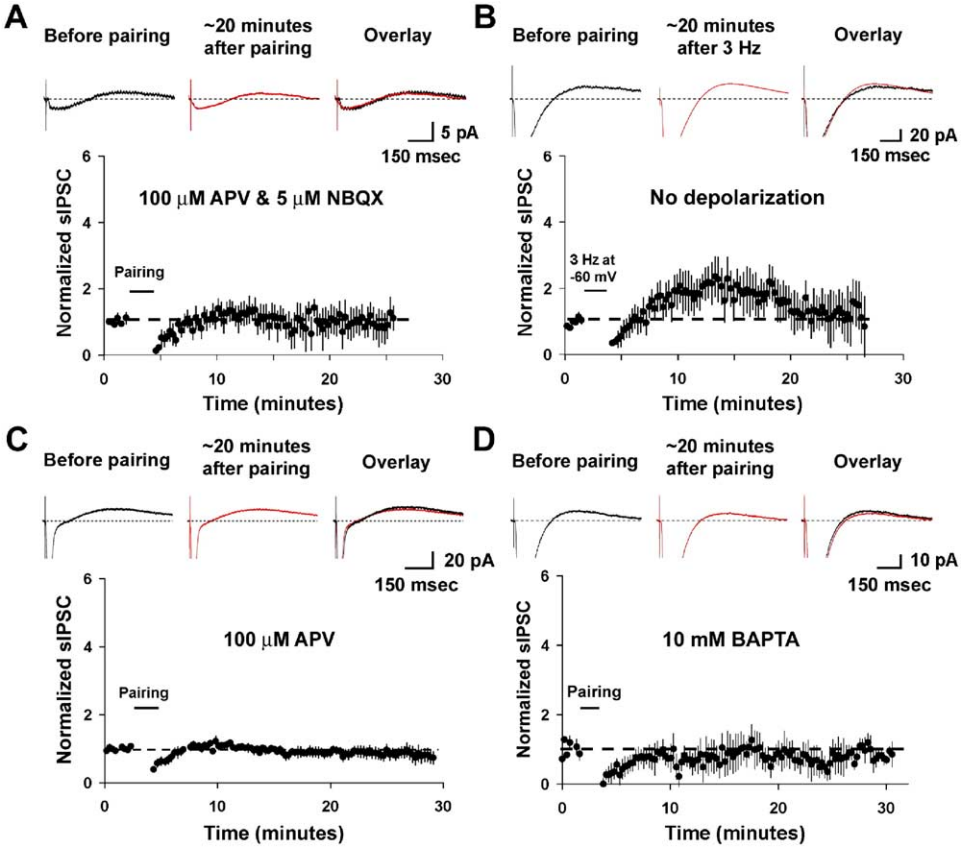

Figure 4. Postsynaptic Ca^{2+} and NMDA-R Activity Are Necessary for Inducing LTP of sIPSC

(A) Treatment of slice culture with APV as well as NBQX reduced both EPSC and sIPSC amplitudes and eliminated LTP of sIPSC (n = 7, p = 0.1).

(B) Three hertz stimulation without concurrent postsynaptic depolarization failed to induce sustained potentiation of sIPSC (n = 6, p = 0.1).

(C) Treatment with the NMDA-R antagonist APV but not the AMPA-R antagonist NBQX eliminated LTP of sIPSC (n = 6, p = 0.3) while preserving its size.

(D) Chelating postsynaptic Ca^{2+} with 10 mM BAPTA in the pipette solution abolished LTP of sIPSC (n = 6, p = 0.6).

ing the postsynaptic pyramidal neuron and found that, analogous to our observations with the acute slice (Figure 3F), there was no persistent potentiation of the sIPSC (123% ± 26% at ~20 min after pairing, n = 6, p = 0.1) (Figure 4B). Second, when we treated the cultured slices only with antagonists of the $GABA_A$-Rs and NMDA-Rs, there was no pairing-induced potentiation of the biphasic response composed of AMPA-R-mediated EPSC (AMPA-R EPSC) and the sIPSC (90% ± 12%, n = 6, p = 0.3) (Figure 4C). These experiments confirm that NMDA-R activation via the pairing protocol is required for LTP of the sIPSC.

Induction of the sIPSC LTP Is Dependent on Postsynaptic Ca^{2+} Increase

To ask whether sIPSC potentiation is due to Ca^{2+} influx through NMDA-Rs, we tested the effect of chelating internal Ca^{2+} and blocking Ca^{2+} channels and whether LTP of sIPSC is induced locally near the activated synapses on dendrites. Whereas the pairing protocol still caused LTP of sIPSC when the intracellular Ca^{2+} level was moderately buffered by 1.1 mM EGTA, no potentiation of sIPSC could be induced with 10 mM BAPTA in the patch pipette solution (87% ± 19% at ~20 min after pairing, n = 6, p = 0.6) (Figure 4D). A rise in postsynaptic Ca^{2+} is likely responsible for potentiating the sIPSC since Oregon green BAPTA 488-1 or lucifer yellow—fluorescent markers of sizes comparable to BAPTA—could diffuse from the pipette solution to distal apical dendrites within 5–10 min after whole-cell patch-clamp was established (Figure S2). Blocking voltage-gated Ca^{2+} channels with nifedipine (100 μM), however, did not eliminate pairing-induced LTP of sIPSC (295% ± 53% at ~20 min after pairing, n = 7, p < 0.01; Figure S3). Moreover, pairing depolarization with stimulation of nerve fibers near proximal dendrites (pathway 2) did not cause potentiation of sIPSC elicited by nerve stimulation near distal dendrites (pathway 1) of CA1 pyramidal neurons (107% ± 26% at ~20 min after pairing for pathway 2, n = 8, p = 0.2; Figure S4). Taken together, these findings suggest that Ca^{2+} influx through NMDA-Rs is essential for the induction of LTP of sIPSC.

Even though pairing-induced potentiation of the sIPSC requires postsynaptic NMDA-R activation and Ca^{2+} rise, a priori, it remains possible that this potentiation could result from increased GABA release, perhaps by retrograde signaling via endocannabinoids (Chevaleyre and Castillo, 2003; Piomelli, 2003; Wilson and Nicoll, 2001). However, the CB1 cannabinoid-receptor antagonist AM251 (2 μM) did not affect pairing-induced

LTP of sIPSC (370% ± 33% at ~20 min after pairing, n = 5, p < 0.001). Moreover, the pairing protocol did not alter GABA release to an extent that affected the paired-pulse ratio of the $GABA_A$-R mediated fIPSC (before pairing, 0.74 ± 0.04; 10 min after pairing, 0.74 ± 0.05, p = 0.9; 20 min after pairing, 0.70 ± 0.04, p = 0.5; n = 5); the paired-pulse ratio's sensitivity to transmitter release was verified by varying Ca^{2+} concentrations in control experiments. Thus, the pairing-induced LTP of sIPSC could not be attributed to CB1 receptor-mediated endocannabinoid retrograde signaling or increased GABA release.

Activation of CaMKII Is Necessary and Sufficient for Inducing sIPSC Potentiation

CaMKII activity is necessary for sIPSC potentiation because treatment of the slice culture with 10 μM KN-93, a selective inhibitor of CaMKII, eliminated pairing-induced LTP of sIPSC (90% ± 15% at ~20 min after pairing, n = 11, p = 0.6) (Figure 5A). To ask whether postsynaptic CaMKII activity is also sufficient for sIPSC potentiation, we utilized the Sindbis virus to introduce into CA1 pyramidal neurons the constitutively active enzyme fused with EGFP, CaMKII(1–290)-EGFP; the great majority of the infected neurons were glutamatergic pyramidal neurons. For internal control, we simultaneously recorded from an uninfected neuron and a nearby neuron expressing CaMKII(1–290)-EGFP (Figure 5B) and compared their sIPSCs that were elicited with the same condition for synaptic stimulation.

The constitutively active CaMKII potentiated the sIPSC (neurons expressing CaMKII(1–290)-EGFP, 6.1 ± 0.5 pA; neighboring control neurons, 3.0 ± 1.0 pA; n = 16, p < 0.0005) but not the NMDA-R EPSC (neurons expressing CaMKII(1–290)-EGFP, 46.0 ± 10.7 pA; neighboring control neurons, 47.5 ± 12.5 pA; n = 17, p = 0.4) (Figure 5D). In control experiments, neurons expressing EGFP and their neighboring uninfected neurons yielded similar sIPSC (neurons expressing EGFP, 2.9 ± 0.7 pA; neighboring control neurons, 3.1 ± 0.9 pA; n = 18, p = 0.8) and NMDA-R EPSC (neurons expressing EGFP, 38.8 ± 5.1 pA; neighboring control neurons, 40.9 ± 6.0 pA; n = 24, p = 0.4) (Figure 5C). Not only was constitutively active CaMKII sufficient for potentiating the sIPSC, it occluded pairing-induced LTP of sIPSC; neurons expressing CaMKII(1–290)-EGFP showed no further potentiation of sIPSC after pairing (113% ± 54%, n = 7, p = 0.1), while control neurons expressing EGFP still exhibited pairing-induced LTP of sIPSC (287% ± 43%, n = 4, p < 0.01) (Figure 5E). These experiments demonstrate that sIPSC was potentiated by the activation of CaMKII in the postsynaptic CA1 pyramidal neurons.

The Nova-2 RNA Binding Protein Is Essential for Pairing-Induced sIPSC Potentiation

Having established that the sIPSC mediated by $GABA_B$-Rs and GIRK channels can be potentiated by activation of NMDA-Rs and CaMKII in CA1 pyramidal neurons, we wondered whether this synaptic plasticity of slow inhibition might be subjected to concerted modulation of relevant synaptic proteins. One candidate for coordinating such modulation is Nova-2 because it regulates a network of synaptic proteins and one-third of its targets are molecules involved in inhibitory synaptic transmission, including $GABA_B$-Rs and GIRK channels (Ule et al., 2003, 2005).

To characterize synaptic transmission and plasticity in the Nova-2 null mice (Ule et al., 2003) (Figure S5), which lived for 2–3 weeks after birth, we first measured the resting membrane potential of CA1 pyramidal neurons in hippocampal slice culture and found no difference between Nova-2 null mice (–60.6 ± 3.5 mV, n = 8) and their heterozygous siblings (–59.4 ± 3.1 mV, n = 5, p = 0.5). Next, we examined the miniature EPSCs and found no effect of the null mutation on the amplitude (*Nova-2*$^{-/-}$, 3.5 ± 0.3 pA; *Nova-2*$^{+/-}$, 3.9 ± 0.6 pA; n = 7, p = 0.5) or frequency (*Nova-2*$^{-/-}$, 0.5 ± 0.2 Hz; *Nova-2*$^{+/-}$, 0.4 ± 0.2 Hz; n = 7, p = 0.7) of these unitary responses (Figure 6A). We also found similar ratios of AMPA-R EPSC measured at –60 mV and NMDA-R EPSC at +40 mV (*Nova-2*$^{-/-}$, 2.3 ± 0.9, n = 8; *Nova-2*$^{+/-}$, 2.5 ± 0.8, n = 7; p = 0.9) (Figure 6B). Moreover, when we recorded the NMDA-R-mediated EPSC at different membrane potentials in the presence of the AMPA-R antagonist NBQX, we found comparable voltage dependence of the NMDA-R EPSC in Nova-2 null mutants and their heterozygous sib controls (Figure 6C). Finally, the pairing protocol elicited LTP of EPSC in both heterozygous control mice (pairing pathway, 171% ± 14%, n = 10, p < 0.01; control pathway, 99% ± 8%, n = 5, p = 0.8) and Nova-2 null mice (pairing pathway, 177% ± 14%, n = 9, p < 0.01; control pathway, 99% ± 13%, n = 4, p = 0.9) (Figure 6D). These experiments thus revealed no significant differences between Nova-2 null mice and control mice in excitatory synaptic transmission.

To test whether Nova-2 function is important for inhibitory synaptic transmission, we compared the null mutants with their heterozygous siblings and found no difference in the miniature fIPSC amplitude (*Nova-2*$^{-/-}$, 5.3 ± 0.4 pA; *Nova-2*$^{+/-}$, 5.2 ± 0.7 pA; n = 5, p = 0.8) or frequency (*Nova-2*$^{-/-}$, 1.4 ± 0.3 Hz; *Nova-2*$^{+/-}$, 1.6 ± 0.4 Hz; n = 5, p = 0.4) (Figure 7A). Moreover, we observed similar ratios of the sIPSC and fIPSC amplitudes, over a wide range of stimulation strength, in the null mutants and their heterozygous siblings (*Nova-2*$^{-/-}$, 0.07 ± 0.02; *Nova-2*$^{+/-}$, 0.08 ± 0.02; n = 8, p = 0.2) (Figure 7B). Finally, in cultured slices treated with NBQX and picrotoxin to block AMPA-Rs and $GABA_A$-Rs, the ratio of the sIPSC and NMDA-R EPSC amplitudes was also normal in the null mutants (*Nova-2*$^{-/-}$, 0.5 ± 0.1; *Nova-2*$^{+/-}$, 0.4 ± 0.1; n = 15, p = 0.4) (Figure 7C).

Interestingly, whereas their heterozygous siblings yielded normal pairing-induced potentiation of sIPSC (338% ± 39% at ~20 min after pairing, n = 6, p < 0.01), the Nova-2 null mutants exhibited no pairing-induced LTP of the sIPSC (130% ± 38% at ~20 min after pairing, n = 8, p = 0.5) (Figure 7D). Since the basal synaptic transmission appeared normal for excitation (Figures 6A and 6B) and inhibition (Figures 7A and 7B) and the capacity of inducing LTP of the EPSC remained in the Nova-2 null mutant (Figure 6D), it appears that the machinery essential for potentiating the slow synaptic inhibition mediated by the $GABA_B$-Rs and GIRK channels is specifically impaired in Nova-2 null mice.

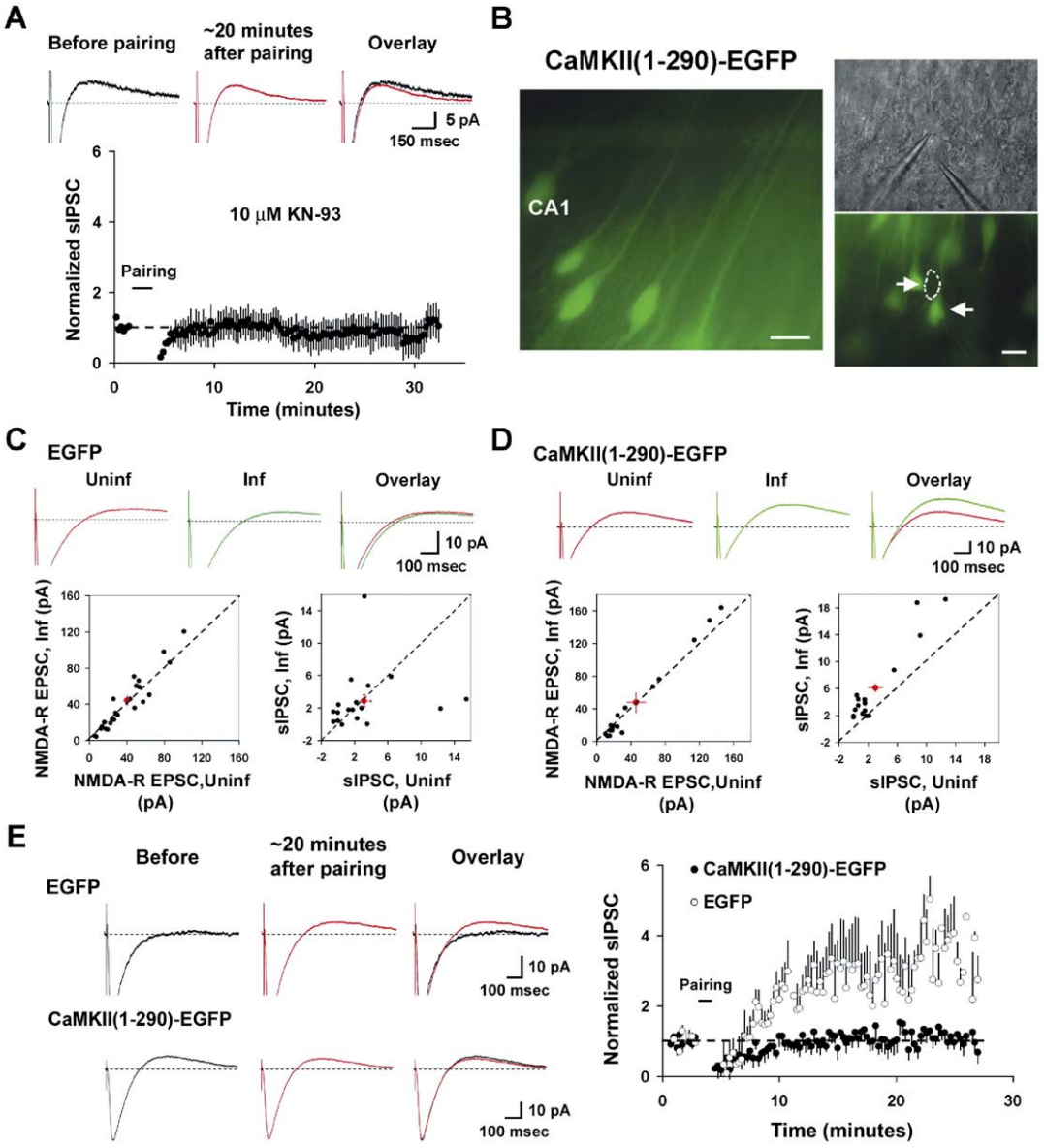

Figure 5. CaMKII Activity Is Necessary and Sufficient for Inducing LTP of sIPSC

(A) The CaMKII inhibitor KN-93 prevented pairing-induced sIPSC potentiation (n = 11, p = 0.6).

(B) Images of CA1 neurons expressing CaMKII(1–290)-EGFP (left) and pairwise recording from one infected neuron and a nearby uninfected neuron (dotted outline) visualized with transmitted light (upper right) and epifluorescence (lower right). Scale bars: 25 μm.

(C) Pairwise comparison between control infected neurons expressing EGFP and nearby uninfected neurons revealed no difference in sIPSC (n = 18, p = 0.8) or NMDAR-EPSC (n = 24, p = 0.4).

(D) Expression of constitutively active CaMKII(1–290)-EGFP potentiated sIPSC (n = 16, p < 0.0005) but not NMDA-R EPSC (n = 17, p = 0.4).

(E) No further potentiation of sIPSC in neurons expressing CaMKII(1–290)-EGFP (n = 7, p = 0.1), in contrast to control neurons expressing EGFP (n = 4, p < 0.01).

Discussion

Neurotransmitters not only induce rapid potential changes in the millisecond timescale via ionotropic receptors, they activate G protein-coupled metabotropic receptors to influence neuronal activity for seconds if not minutes (Hille, 2001). Moreover, the metabotropic receptors' ability to respond to transmitters released at a distance allows neurons to integrate and process multiple synaptic inputs. Prompted by the unexpected localization of both $GABA_B$-Rs and GIRK channels to the dendritic spines (Drake et al., 1997; Kulik et al., 2003)—where excitatory synapses reside and LTP of EPSC could be induced—our study uncovered a new form of synaptic plasticity, LTP of sIPSC mediated by $GABA_B$-Rs and GIRK channels (Figure 2), due to activation of NMDA-Rs as the coincidence detector (Figures 4A–4C).

In addition to identifying the mechanism common to LTP of EPSC and LTP of sIPSC, we came upon regulatory machinery specific for the synaptic plasticity of slow inhibition. Like LTP of EPSC (Malenka et al., 1988,

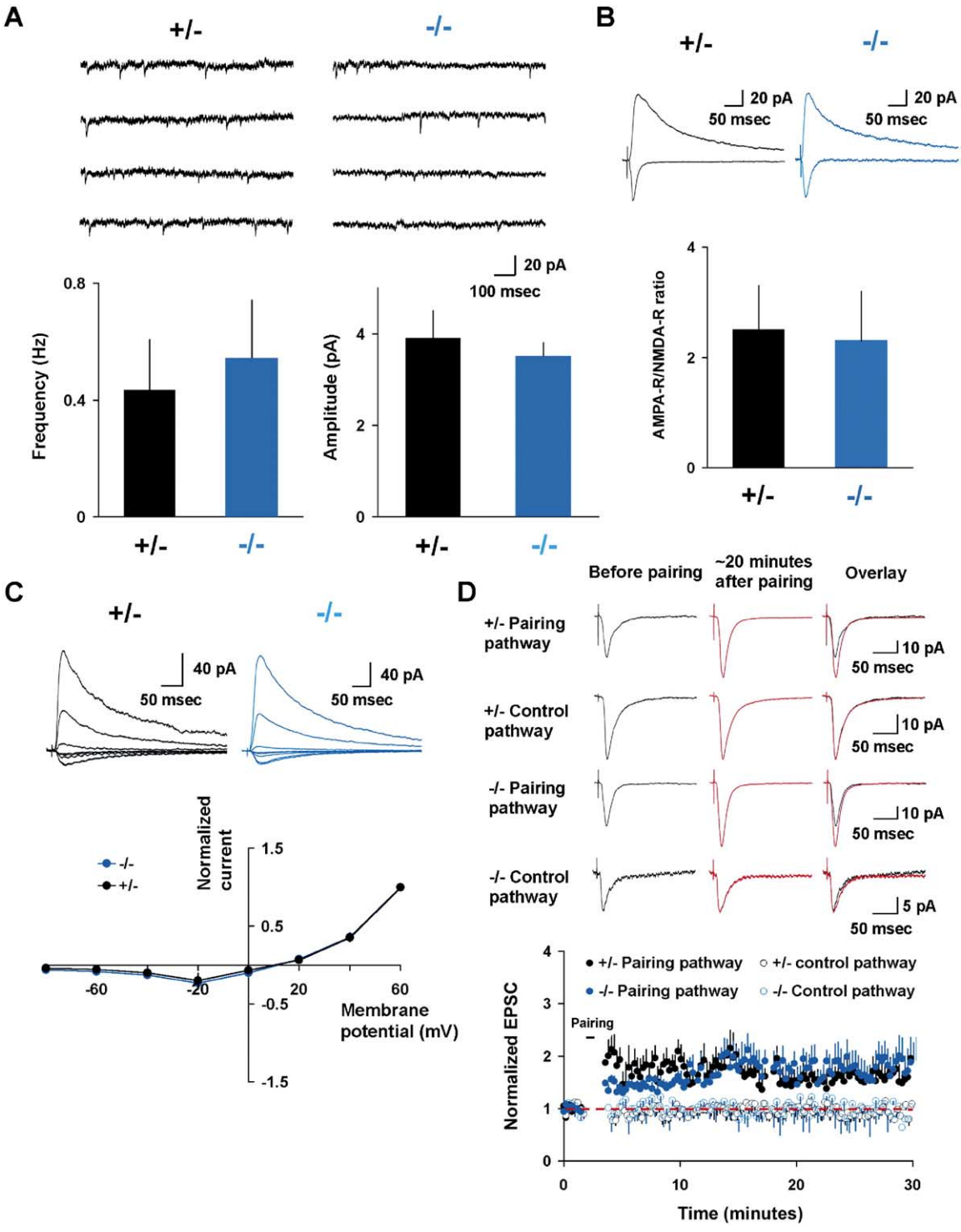

Figure 6. Nova-2 Null Mice Exhibit Excitatory Synaptic Responses and LTP of EPSC Similar to those of Their Heterozygous Siblings

(A) The miniature EPSC of Nova-2 null mice (–/–) exhibited amplitude (n = 7, p = 0.5) and frequency (n = 7, p = 0.7) (blue) similar to those of heterozygous siblings (+/–) (black). The same color label is used in subsequent panels and figures.

(B) The ratio of AMPA-R EPSC and NMDA-R EPSC was comparable between Nova-2 null mice and heterozygous siblings (n = 8, p = 0.9).

(C) The voltage dependence of NMDA-R EPSC was comparable between Nova-2 null mice and heterozygous siblings (n = 6, p = 0.2).

(D) Similar pairing-induced LTP of EPSC in Nova-2 null mice and their heterozygous siblings.

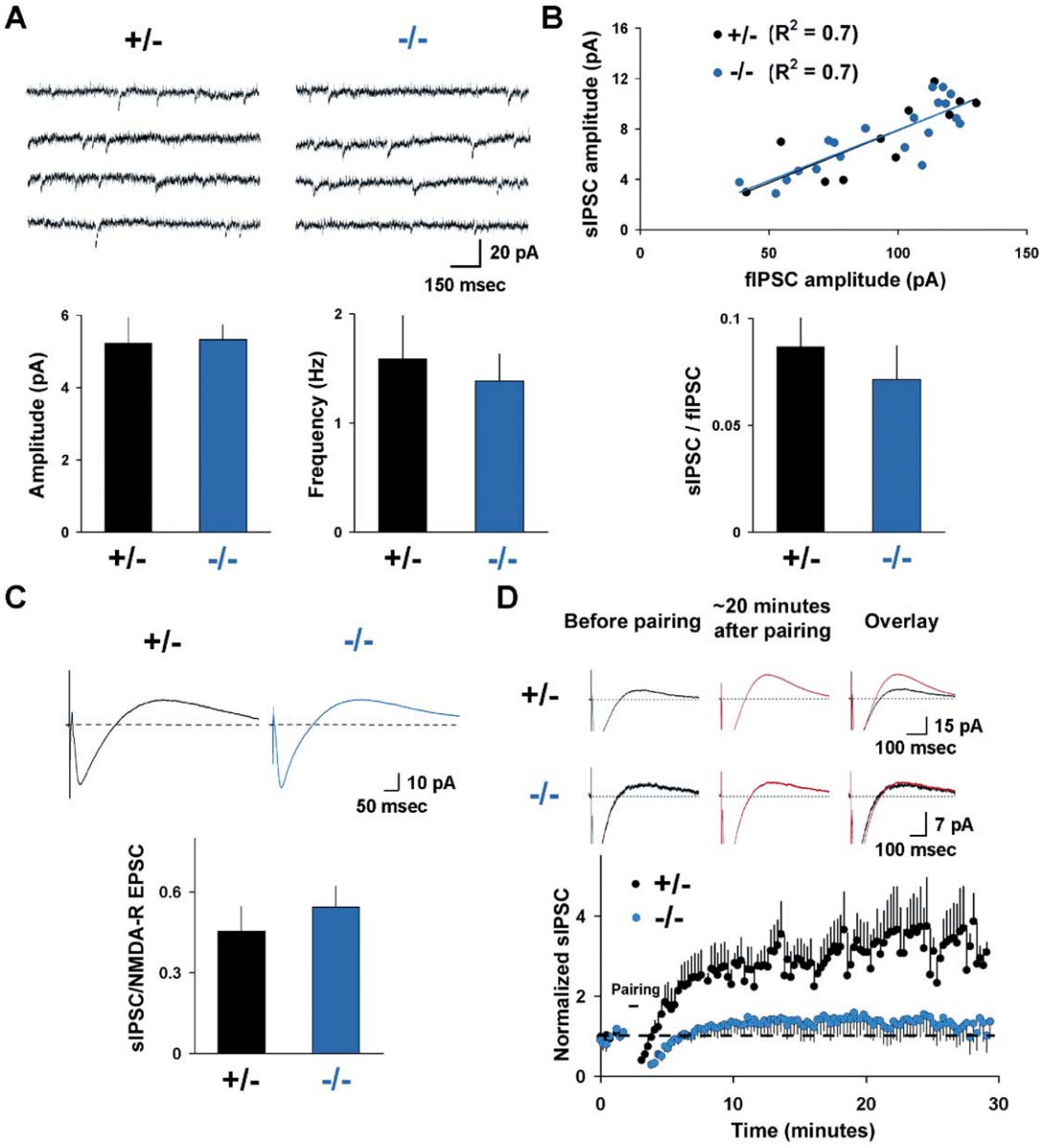

Figure 7. Nova-2 Null Mice with Normal Basal Inhibitory Synaptic Responses, as Compared with Heterozygous Controls, Fail to Show Pairing-Induced LTP of sIPSC

(A) The miniature fIPSC of Nova-2 null mice (–/–) showed normal amplitude (n = 5, p = 0.8) and frequency (n = 5, p = 0.4).
(B) The ratio of sIPSC and fIPSC in Nova-2 null mice (n = 8) was similar to that in control mice (+/–) (n = 8, p = 0.2).
(C) The ratio of sIPSC and NMDA-R EPSC in Nova-2 null mutants (n = 15) was comparable to that in control mice (n = 15, p = 0.4).
(D) Nova-2 null mice exhibited no pairing-induced sIPSC potentiation (n = 8, p = 0.5), while their heterozygous siblings showed pairing-induced sIPSC LTP (n = 6, p < 0.01).

1989; Malinow et al., 1989), LTP of sIPSC requires postsynaptic Ca^{2+} rise (Figure 4D) and CaMKII activity (Figure 5A). Moreover, expression of constitutively active CaMKII in CA1 pyramidal neurons was sufficient to potentiate sIPSC (Figure 5D) and to occlude pairing-induced LTP of sIPSC (Figure 5E). Remarkably, LTP of sIPSC but not EPSC was absent in the Nova-2 null mice (Figures 6 and 7), raising the intriguing possibility that one of the physiological functions of the Nova-2 RNA binding protein is to enable central neurons to adjust their slow synaptic inhibition based on neuronal activity.

Long-Term Potentiation of Slow Synaptic Inhibition Could Sharpen the Coincidence Detection of Excitatory Synaptic Inputs

One potential consequence of sIPSC potentiation is to narrow the time window for the coincidence detection of excitatory inputs; late-arriving synaptic inputs would be rendered less effective because of the hyperpolarization and increased membrane conductance accompanying the potentiated sIPSC. Importantly, in small structures like the dendritic spines, slow synaptic inhibition mediated by K^+ channel activation via $GABA_B$-Rs is likely to be more effective in dampening the excit-

atory inputs—in principle—than the fast synaptic inhibition, since Cl^- influx through $GABA_A$-Rs into small structures could significantly increase the concentration and hence decrease the driving force for Cl^- (Qian and Sejnowski, 1990). Thus, the localization of both $GABA_B$-Rs and GIRK channels in dendritic spines (Figure 1A) (Drake et al., 1997; Kulik et al., 2003) not only enables the same signaling pathway for synaptic plasticity of excitatory synaptic potentials to induce long-lasting changes of slow synaptic inhibition, potentiation of slow inhibition due to GIRK channel activity also represents one highly effective way of harnessing excitatory synaptic inputs.

In addition to reducing excitation at dendritic spines, slow synaptic inhibition may also induce failures of action-potential propagation along axons, particularly at axonal branch points (Debanne, 2004; Debanne et al., 1997; Kopysova and Debanne, 1998). Thus, potentiation of sIPSC could sharpen the coincidence detection of synchronous excitatory synaptic inputs, a hallmark for learning and memory, in a variety of ways—by reducing the impact of late-arriving excitatory inputs within the spines that receive the synaptic excitation and by decreasing the likelihood that excitation by late-arriving synaptic inputs will be productive in causing transmitter release from the nerve terminals.

Long-term potentiation of slow synaptic inhibition may also modulate rhythmic activities such as the theta oscillation (4–7 Hz), which is important for learning and memory (Hyman et al., 2003; O'Keefe, 1993; Sederberg et al., 2003; Seidenbecher et al., 2003). Interneurons are remarkably effective in synchronizing this oscillatory firing pattern of hippocampal pyramidal neurons (Cobb et al., 1995). It is of interest to note that GABA-uptake blocker causes a decrease in the oscillation frequency, which can be reversed by blockade of $GABA_B$-Rs (Scanziani, 2000). If theta modulation indeed depends on postsynaptic $GABA_B$-Rs, LTP of sIPSC is likely to slow theta oscillation and hence shift its phase, a crucial temporal parameter in filtering out specific synaptic activities for potentiation or depression (Hyman et al., 2003).

Nova-2 Functions and Synaptic Plasticity of Slow Inhibition

Nova proteins bind to known sequence motifs in the RNA with high affinity to regulate alternative splicing and may also associate with other RNA sequences in exons (Dredge and Darnell, 2003; Dredge et al., 2005; Jensen et al., 2000; Musunuru and Darnell, 2001; Ule et al., 2003, 2005). As paraneoplastic neurologic disease antigens, these RNA binding proteins are probably responsible for the reduced inhibitory control of movements and dementia in POMA patients (Albert and Darnell, 2004; Buckanovich et al., 1993; Hormigo et al., 1994; Pranzatelli, 1992; Yang et al., 1998). Interestingly, many RNAs that are Nova-2 targets code for proteins that mediate synaptic inhibition, including $GABA_B$-Rs and GIRK channels (Ule et al., 2003, 2005). The ability of hippocampal neurons from Nova-2 null mice to exhibit LTP of EPSC (Figure 6) but not sIPSC (Figure 7) strongly suggests that Nova-2 functions specifically in the machinery that endows slow synaptic inhibition with the capacity to respond to NMDA-R activation with long-lasting changes.

How might Nova-2 contribute to synaptic plasticity of slow inhibition? Multiple variants for both $GABA_B$-R and GIRK channels exist due to alternative splicing (Isomoto et al., 1998; Martin et al., 2001; Pfaff et al., 1999; Wei et al., 1998) or alternative promoter usage (Steiger et al., 2004) to diversify their function and their traffic pattern (Charles et al., 2001; Ma et al., 2002; Martin et al., 2004). As an RNA binding protein known to regulate splicing of molecules important for synaptic transmission and plasticity (Ule et al., 2005), Nova-2 may function in CA1 pyramidal neurons to dictate appropriate representations of the splice variants of $GABA_B$-Rs, GIRK channels, or other associated molecules (Couve et al., 2001, 2004; Nehring et al., 2000; Vernon et al., 2001; White et al., 2000), perhaps to ensure that these molecules in dendritic spines and other synaptic sites are suitably equipped to respond to signaling downstream of the coincidence detector, the NMDA-R. While altered splicing patterns are evident from analyses of different regions of the brain and spinal cord from Nova-1 and Nova-2 null mice (Dredge and Darnell, 2003; Jensen et al., 2000; Ule et al., 2005), further studies will be necessary to uncover cell-type-specific functions of Nova proteins. In this regard, it is worth noting that regulation of splicing of various K^+ channels and Ca^{2+} channels in individual neurons, or specific subsets of neurons, plays physiologically important roles in fine tuning excitability (Baranauskas et al., 2003; Bell et al., 2004; Fettiplace and Fuchs, 1999). Whereas Nova proteins are known to regulate alternative splicing, given the intriguing coupling between RNA splicing and cytoplasmic RNA targeting and regulation (Gu et al., 2002; Hachet and Ephrussi, 2004; Kataoka et al., 2000; Palacios, 2002), a physiological role of Nova-2 outside the nucleus—in neuronal soma or processes—remains an interesting possibility for future studies.

Experimental Procedures

Immunocytochemistry

Primary cultures of rat hippocampal neurons (Brewer et al., 1993) were transfected with EGFP constructs, fixed with 4% paraformaldehyde/4% sucrose in phosphate-buffered saline at 4°C for 20 min, and exposed to GIRK2 antibodies (Alomone, Jerusalem, Israel) for immunofluorescence.

Hippocampal Organotypic Slice Culture and Electrophysiology

Rat hippocampal organotypic slice cultures (Hayashi et al., 2000) in a recording chamber superfused with ACSF solution containing (in mM) 119 NaCl, 2.5 KCl, 4 $CaCl_2$, 4 $MgCl_2$, 26.2 $NaHCO_3$, 1 NaH_2PO_4, 11 glucose and equilibrated with 5% CO_2/95% O_2 were used for whole-cell recordings at room temperature from CA1 pyramidal neurons with patch electrodes (3–5 MΩ) filled with pipette solution containing (in mM) 140 K-gluconate, 5 HEPES, 2 $MgCl_2$, 1.1 EGTA, 2 MgATP, 3 Na_3GTP. Recordings were amplified with Axonpatch 1D, filtered at 1 kHz, and sampled using programs written in Igor (Wavematrics, Lake Oswego, Oregon). To evoke synaptic responses, a cluster electrode (FHC, Bowdoinham, Maine) was placed 300–500 μm from the stratum pyramidale layer in the CA1 region, and stimuli of ~0.1 msec duration were delivered. Data were analyzed using macros written in Igor and Microsoft Excel. Sindbis viruses and the CaMKII(1–290)-EGFP construct were constructed as reported (Hayashi et al., 2000), and recordings were made 24 to 36 hr after neurons were infected. Recordings from cell

pairs were performed with neurons whose somata were within ~20 μm, one showing EGFP fluorescence and the other not. For recording miniature fIPSC at −70 mV and miniature EPSC at −60 mV, the patch pipette was filled with the internal solution containing (in mM) 115 cesium methanesulfonate, 20 CsCl, 10 HEPES, 2.5 $MgCl_2$, 4 Na_2ATP, 0.4 Na_3GTP, 10 sodium phosphocreatine, 0.6 EGTA (pH 7.25). The external solution contained the sodium-channel blocker TTX (2 μM) and blockers for glutamate receptors (5 μM NBQX and 100 μM APV) (for recording miniature fIPSC) or $GABA_A$-R (100 μM picrotoxin) (for recording miniature EPSC). All recording was done at room temperature. The amplitudes of AMPA-R and NMDA-R EPSC were measured with an average of a 10–15 msec window at the peak (at −60 mV) and ~200 msec (at +40 mV) from the onset of the synaptic currents, respectively. Drugs used were NBQX, picrotoxin, SCH23390, SCH50911, AM251, and APV (Tocris, Ellisville, Missouri); tertiapin (Alomone); and KN-93 (Calbiochem, San Diego, California). Data are expressed as means ± SEM, and statistical differences were determined using Student's t test and nonparametric Mann-Whitney or Wilcoxon tests.

Acute Hippocampal Slice

Brains from 25- to 30-day-old Sprague-Dawley rats (Charles River, Wilmington, Massachusetts) were removed and immersed in cold buffer containing (in mM) 87 NaCl, 25 $NaHCO_3$, 75 sucrose, 10 glucose, 2.5 KCl, 1 NaH_2PO_4, 0.5 $CaCl_2$, 7 $MgCl_2$ and equilibrated with 95% O_2/5% CO_2. Hippocampal slices ~400 μm thick were prepared with Leica VT1000s vibratome; transferred to a holding chamber with the ACSF solution containing (in mM) 119 NaCl, 2.5 KCl, 2.5 $CaCl_2$, 1.3 $MgCl_2$, 26.2 $NaHCO_3$, 1 NaH_2PO_4, 11 glucose and bubbled with 95%O_2/5% CO_2 at 37°C for ~1 hr; and then incubated at room temperature for at least 30 min before recording.

Nova-2 Mice

Hippocampal organotypic slice cultures were prepared from heterozygous and homozygous sibling mice with the same procedure as for rat slice culture. Two pairs of primers designed to target the wild-type locus and the mutant locus, respectively, were used for genotyping: (1) 5′-GGATCCTCTAGAGTCACACC-3′ and 5′-GGGTGACATGGAAGAAAGGG-3′ and (2) 5′-TTTCCGTCTCTGGTGTAGC-3′ and 5′-GTGCACACACACATGTCC-3′. A band size of 450 bp is expected for the wild-type locus, and a band size of 550 bp is expected for the mutant locus.

Supplemental Data

Supplemental Data include five figures and can be found with this article online at http://www.cell.com/cgi/content/full/123/1/105/DC1/.

Acknowledgments

We are grateful to Dr. Roger A. Nicoll for his generosity in providing thoughtful inputs, technical advice, and access to lab equipment. We thank Dr. Steve A. Siegelbaum for advice on slice physiology involving perforant-path inputs and Jan lab members for helpful discussions. We acknowledge the NIH grant support RO1 NS34389 and NS40955 to R.B.D., NS047200 to Y.N.J., and MH63981 to L.Y.J. in the Silvio Conte Center of Neuroscience at UCSF. M.R. is partly funded by a fellowship from Human Frontier Science Program, and S.-H.S. is supported by a Helen Hay Whitney fellowship and was a Howard Hughes Medical Institute (HHMI) research associate. R.B.D., Y.N.J., and L.Y.J. are HHMI investigators.

Received: April 2, 2005
Revised: July 3, 2005
Accepted: July 28, 2005
Published: October 6, 2005

References

Albert, M.L., and Darnell, R.B. (2004). Paraneoplastic neurological degenerations: keys to tumour immunity. Nat. Rev. Cancer *4*, 36–44.

Anikstejn, L., and Ben-Ari, Y. (1995). Expression of LTP by AMPA and/or NMDA receptors is determined by the extent of NMDA receptors activation during the tetanus. J. Neurophysiol. *74*, 2349–2357.

Baranauskas, G., Tkatch, T., Nagata, K., Yeh, J.Z., and Surmeier, D.J. (2003). Kv3.4 subunits enhance the repolarizing efficiency of Kv3.1 channels in fast-spiking neurons. Nat. Neurosci. *6*, 258–266.

Bashir, Z.I., Alford, S., Davies, S.N., Randall, A.D., and Collingridge, G.L. (1991). Long-term potentiation of NMDA receptor-mediated synaptic transmission in the hippocampus. Nature *349*, 156–158.

Bell, T.J., Thaler, C., Castiglioni, A.J., Helton, T.D., and Lipscombe, D. (2004). Cell-specific alternative splicing increases calcium channel current density in the pain pathway. Neuron *41*, 127–138.

Bichet, D., Lin, Y.F., Ibarra, C.A., Huang, C.S., Yi, B.A., Jan, Y.N., and Jan, L.Y. (2004). Evolving potassium channels by means of yeast selection reveals structural elements important for selectivity. Proc. Natl. Acad. Sci. USA *101*, 4441–4446.

Bliss, T.V., and Collingridge, G.L. (1993). A synaptic model of memory: long-term potentiation in the hippocampus. Nature *361*, 31–39.

Bolser, D.C., Blythin, D.J., Chapman, R.W., Egan, R.W., Hey, J.A., Rizzo, C., Kuo, S.C., and Kreutner, W. (1995). The pharmacology of SCH 50911: a novel, orally-active GABA-beta receptor antagonist. J. Pharmacol. Exp. Ther. *274*, 1393–1398.

Brewer, G.J., Torricelli, J.R., Evege, E.K., and Price, P.J. (1993). Optimized survival of hippocampal neurons in B27-supplemented Neurobasal, a new serum-free medium combination. J. Neurosci. Res. *35*, 567–576.

Buckanovich, R.J., Posner, J.B., and Darnell, R.B. (1993). Nova, the paraneoplastic Ri antigen, is homologous to an RNA-binding protein and is specifically expressed in the developing motor system. Neuron *11*, 657–672.

Charles, K.J., Evans, M.L., Robbins, M.J., Calver, A.R., Leslie, R.A., and Pangalos, M.N. (2001). Comparative immunohistochemical localisation of GABA(B1a), GABA(B1b) and GABA(B2) subunits in rat brain, spinal cord and dorsal root ganglion. Neuroscience *106*, 447–467.

Chevaleyre, V., and Castillo, P.E. (2003). Heterosynaptic LTD of hippocampal GABAergic synapses: a novel role of endocannabinoids in regulating excitability. Neuron *38*, 461–472.

Cobb, S.R., Buhl, E.H., Halasy, K., Paulsen, O., and Somogyi, P. (1995). Synchronization of neuronal activity in hippocampus by individual GABAergic interneurons. Nature *378*, 75–78.

Collingridge, G.L., Herron, C.E., and Lester, R.A. (1988). Synaptic activation of N-methyl-D-aspartate receptors in the Schaffer collateral-commissural pathway of rat hippocampus. J. Physiol. *399*, 283–300.

Couve, A., Kittler, J.T., Uren, J.M., Calver, A.R., Pangalos, M.N., Walsh, F.S., and Moss, S.J. (2001). Association of GABA(B) receptors and members of the 14–3-3 family of signaling proteins. Mol. Cell. Neurosci. *17*, 317–328.

Couve, A., Restituito, S., Brandon, J.M., Charles, K.J., Bawagan, H., Freeman, K.B., Pangalos, M.N., Calver, A.R., and Moss, S.J. (2004). Marlin-1, a novel RNA-binding protein associates with GABA receptors. J. Biol. Chem. *279*, 13934–13943.

Daw, N.W., Stein, P.S., and Fox, K. (1993). The role of NMDA receptors in information processing. Annu. Rev. Neurosci. *16*, 207–222.

Debanne, D. (2004). Information processing in the axon. Nat. Rev. Neurosci. *5*, 304–316.

Debanne, D., Guerineau, N.C., Gahwiler, B.H., and Thompson, S.M. (1997). Action-potential propagation gated by an axonal I(A)-like K+ conductance in hippocampus. Nature *389*, 286–289.

Drake, C.T., Bausch, S.B., Milner, T.A., and Chavkin, C. (1997). GIRK1 immunoreactivity is present predominantly in dendrites, dendritic spines, and somata in the CA1 region of the hippocampus. Proc. Natl. Acad. Sci. USA *94*, 1007–1012.

Dredge, B.K., and Darnell, R.B. (2003). Nova regulates GABA(A) receptor gamma2 alternative splicing via a distal downstream UCAU-rich intronic splicing enhancer. Mol. Cell. Biol. *23*, 4687–4700.

Dredge, B.K., Stefani, G., Engelhard, C.C., and Darnell, R.B. (2005). Nova autoregulation reveals dual functions in neuronal splicing. EMBO J. *24*, 1608–1620.

Fettiplace, R., and Fuchs, P.A. (1999). Mechanisms of hair cell tuning. Annu. Rev. Physiol. *61*, 809–834.

Gu, W., Pan, F., Zhang, H., Bassell, G.J., and Singer, R.H. (2002). A predominantly nuclear protein affecting cytoplasmic localization of beta-actin mRNA in fibroblasts and neurons. J. Cell Biol. *156*, 41–51.

Hachet, O., and Ephrussi, A. (2004). Splicing of oskar RNA in the nucleus is coupled to its cytoplasmic localization. Nature *428*, 959–963.

Harris, K.M. (1999). Structure, development, and plasticity of dendritic spines. Curr. Opin. Neurobiol. *9*, 343–348.

Hayashi, Y., Shi, S.H., Esteban, J.A., Piccini, A., Poncer, J.C., and Malinow, R. (2000). Driving AMPA receptors into synapses by LTP and CaMKII: requirement for GluR1 and PDZ domain interaction. Science *287*, 2262–2267.

Hille, B. (1992). G protein-coupled mechanisms and nervous signaling. Neuron *9*, 187–195.

Hille, B. (2001). Ion Channels of Excitable Membranes, Third Edition (Sunderland, MA: Sinauer).

Hormigo, A., Dalmau, J., Rosenblum, M.K., River, M.E., and Posner, J.B. (1994). Immunological and pathological study of anti-Ri-associated encephalopathy. Ann. Neurol. *36*, 896–902.

Hyman, J.M., Wyble, B.P., Goyal, V., Rossi, C.A., and Hasselmo, M.E. (2003). Stimulation in hippocampal region CA1 in behaving rats yields long-term potentiation when delivered to the peak of theta and long-term depression when delivered to the trough. J. Neurosci. *23*, 11725–11731.

Isomoto, S., Kaibara, M., Sakurai-Yamashita, Y., Nagayama, Y., Uezono, Y., Yano, K., and Taniyama, K. (1998). Cloning and tissue distribution of novel splice variants of the rat GABAB receptor. Biochem. Biophys. Res. Commun. *253*, 10–15.

Jensen, K.B., Dredge, B.K., Stefani, G., Zhong, R., Buckanovich, R.J., Okano, H.J., Yang, Y.Y., and Darnell, R.B. (2000). Nova-1 regulates neuron-specific alternative splicing and is essential for neuronal viability. Neuron *25*, 359–371.

Kataoka, N., Yong, J., Kim, V.N., Velazquez, F., Perkinson, R.A., Wang, F., and Dreyfuss, G. (2000). Pre-mRNA splicing imprints mRNA in the nucleus with a novel RNA-binding protein that persists in the cytoplasm. Mol. Cell *6*, 673–682.

Kauer, J.A., Malenka, R.C., and Nicoll, R.A. (1988). A persistent postsynaptic modification mediates long-term potentiation in the hippocampus. Neuron *1*, 911–917.

Kopysova, I.L., and Debanne, D. (1998). Critical role of axonal A-type K+ channels and axonal geometry in the gating of action potential propagation along CA3 pyramidal cell axons: a simulation study. J. Neurosci. *18*, 7436–7451.

Kulik, A., Vida, I., Lujan, R., Haas, C.A., Lopez-Bendito, G., Shigemoto, R., and Frotscher, M. (2003). Subcellular localization of metabotropic GABA(B) receptor subunits GABA(B1a/b) and GABA(B2) in the rat hippocampus. J. Neurosci. *23*, 11026–11035.

Kuzhikandathil, E.V., and Oxford, G.S. (2002). Classic D1 dopamine receptor antagonist R-(+)-7-chloro-8-hydroxy-3-methyl-1-phenyl-2,3,4,5-tetrahydro-1H-3-benzazepine hydrochloride (SCH23390) directly inhibits G protein-coupled inwardly rectifying potassium channels. Mol. Pharmacol. *62*, 119–126.

Liao, Y.J., Jan, Y.N., and Jan, L.Y. (1996). Heteromultimerization of G-protein-gated inwardly rectifying K+ channel proteins GIRK1 and GIRK2 and their altered expression in weaver brain. J. Neurosci. *16*, 7137–7150.

Lisman, J., Schulman, H., and Cline, H. (2002). The molecular basis of CaMKII function in synaptic and behavioural memory. Nat. Rev. Neurosci. *3*, 175–190.

Luque, F.A., Furneaux, H.M., Ferziger, R., Rosenblum, M.K., Wray, S.H., Schold, S.C., Jr., Glantz, M.J., Jaeckle, K.A., Biran, H., Lesser, M., et al. (1991). Anti-Ri: an antibody associated with paraneoplastic opsoclonus and breast cancer. Ann. Neurol. *29*, 241–251.

Lüscher, C., Jan, L.Y., Stoffel, M., Malenka, R.C., and Nicoll, R.A. (1997). G protein-coupled inwardly rectifying K+ channels (GIRKs) mediate postsynaptic but not presynaptic transmitter actions in hippocampal neurons. Neuron *19*, 687–695.

Ma, D., Zerangue, N., Raab-Graham, K., Fried, S.R., Jan, Y.N., and Jan, L.Y. (2002). Diverse trafficking patterns due to multiple traffic motifs in G protein-activated inwardly rectifying potassium channels from brain and heart. Neuron *33*, 715–729.

Malenka, R.C., Kauer, J.A., Zucker, R.S., and Nicoll, R.A. (1988). Postsynaptic calcium is sufficient for potentiation of hippocampal synaptic transmission. Science *242*, 81–84.

Malenka, R.C., Kauer, J.A., Perkel, D.J., Mauk, M.D., Kelly, P.T., Nicoll, R.A., and Waxham, M.N. (1989). An essential role for postsynaptic calmodulin and protein kinase activity in long-term potentiation. Nature *340*, 554–557.

Malinow, R. (2003). AMPA receptor trafficking and long-term potentiation. Philos. Trans. R. Soc. Lond. B Biol. Sci. *358*, 707–714.

Malinow, R., Schulman, H., and Tsien, R.W. (1989). Inhibition of postsynaptic PKC or CaMKII blocks induction but not expression of LTP. Science *245*, 862–866.

Marshall, F.H., Jones, K.A., Kaupmann, K., and Bettler, B. (1999). GABAB receptors - the first 7TM heterodimers. Trends Pharmacol. Sci. *20*, 396–399.

Martin, S.C., Russek, S.J., and Farb, D.H. (2001). Human GABA(B)R genomic structure: evidence for splice variants in GABA(B)R1 but not GABA(B)R2. Gene *278*, 63–79.

Martin, S.C., Steiger, J.L., Gravielle, M.C., Lyons, H.R., Russek, S.J., and Farb, D.H. (2004). Differential expression of gamma-aminobutyric acid type B receptor subunit mRNAs in the developing nervous system and receptor coupling to adenylyl cyclase in embryonic neurons. J. Comp. Neurol. *473*, 16–29.

Musunuru, K., and Darnell, R.B. (2001). Paraneoplastic neurologic disease antigens: RNA-binding proteins and signaling proteins in neuronal degeneration. Annu. Rev. Neurosci. *24*, 239–262.

Nehring, R.B., Horikawa, H.P., El Far, O., Kneussel, M., Brandstatter, J.H., Stamm, S., Wischmeyer, E., Betz, H., and Karschin, A. (2000). The metabotropic GABAB receptor directly interacts with the activating transcription factor 4. J. Biol. Chem. *275*, 35185–35191.

Nicoll, R.A. (2003). Expression mechanisms underlying long-term potentiation: a postsynaptic view. Philos. Trans. R. Soc. Lond. B Biol. Sci. *358*, 721–726.

O'Keefe, J. (1993). Hippocampus, theta, and spatial memory. Curr. Opin. Neurobiol. *3*, 917–924.

Palacios, I.M. (2002). RNA processing: splicing and the cytoplasmic localisation of mRNA. Curr. Biol. *12*, R50–R52.

Pfaff, T., Malitschek, B., Kaupmann, K., Prezeau, L., Pin, J.P., Bettler, B., and Karschin, A. (1999). Alternative splicing generates a novel isoform of the rat metabotropic GABA(B)R1 receptor. Eur. J. Neurosci. *11*, 2874–2882.

Piomelli, D. (2003). The molecular logic of endocannabinoid signalling. Nat. Rev. Neurosci. *4*, 873–884.

Pranzatelli, M.R. (1992). The neurobiology of the opsoclonus-myoclonus syndrome. Clin. Neuropharmacol. *15*, 186–228.

Qian, N., and Sejnowski, T.J. (1990). When is an inhibitory synapse effective? Proc. Natl. Acad. Sci. USA *87*, 8145–8149.

Scanziani, M. (2000). GABA spillover activates postsynaptic GABA(B) receptors to control rhythmic hippocampal activity. Neuron *25*, 673–681.

Sederberg, P.B., Kahana, M.J., Howard, M.W., Donner, E.J., and Madsen, J.R. (2003). Theta and gamma oscillations during encoding predict subsequent recall. J. Neurosci. *23*, 10809–10814.

Seidenbecher, T., Laxmi, T.R., Stork, O., and Pape, H.C. (2003). Amygdalar and hippocampal theta rhythm synchronization during fear memory retrieval. Science *301*, 846–850.

Sheng, M., and Kim, M.J. (2002). Postsynaptic signaling and plasticity mechanisms. Science *298*, 776–780.

Somogyi, P., Tamas, G., Lujan, R., and Buhl, E.H. (1998). Salient features of synaptic organisation in the cerebral cortex. Brain Res. Brain Res. Rev. *26*, 113–135.

Steiger, J.L., Bandyopadhyay, S., Farb, D.H., and Russek, S.J.

(2004). cAMP response element-binding protein, activating transcription factor-4, and upstream stimulatory factor differentially control hippocampal GABABR1a and GABABR1b subunit gene expression through alternative promoters. J. Neurosci. *24*, 6115–6126.

Stein, V., House, D.R., Bredt, D.S., and Nicoll, R.A. (2003). Postsynaptic density-95 mimics and occludes hippocampal long-term potentiation and enhances long-term depression. J. Neurosci. *23*, 5503–5506.

Ule, J., Jensen, K.B., Ruggiu, M., Mele, A., Ule, A., and Darnell, R.B. (2003). CLIP identifies Nova-regulated RNA networks in the brain. Science *302*, 1212–1215.

Ule, J., Ule, A., Spencer, J., Williams, A., Hu, J.S., Cline, M., Wang, H., Clark, T., Fraser, C., Ruggiu, M., et al. (2005). Nova regulates brain-specific splicing to shape the synapse. Nat. Genet. *37*, 844–852. 10.1038/ng1610

Vernon, E., Meyer, G., Pickard, L., Dev, K., Molnar, E., Collingridge, G.L., and Henley, J.M. (2001). GABA(B) receptors couple directly to the transcription factor ATF4. Mol. Cell. Neurosci. *17*, 637–645.

Vida, I., Halasy, K., Szinyei, C., Somogyi, P., and Buhl, E.H. (1998). Unitary IPSPs evoked by interneurons at the stratum radiatum-stratum lacunosum-moleculare border in the CA1 area of the rat hippocampus in vitro. J. Physiol. *506*, 755–773.

Watt, A.J., Sjostrom, P.J., Hausser, M., Nelson, S.B., and Turrigiano, G.G. (2004). A proportional but slower NMDA potentiation follows AMPA potentiation in LTP. Nat. Neurosci. *7*, 518–524.

Wei, J., Hodes, M.E., Piva, R., Feng, Y., Wang, Y., Ghetti, B., and Dlouhy, S.R. (1998). Characterization of murine Girk2 transcript isoforms: structure and differential expression. Genomics *51*, 379–390.

White, J.H., McIllhinney, R.A., Wise, A., Ciruela, F., Chan, W.Y., Emson, P.C., Billinton, A., and Marshall, F.H. (2000). The GABAB receptor interacts directly with the related transcription factors CREB2 and ATFx. Proc. Natl. Acad. Sci. USA *97*, 13967–13972.

Wickman, K., Karschin, C., Karschin, A., Picciotto, M.R., and Clapham, D.E. (2000). Brain localization and behavioral impact of the G-protein-gated K+ channel subunit GIRK4. J. Neurosci. *20*, 5608–5615.

Wilson, R.I., and Nicoll, R.A. (2001). Endogenous cannabinoids mediate retrograde signalling at hippocampal synapses. Nature *410*, 588–592.

Yamada, M., Inanobe, A., and Kurachi, Y. (1998). G protein regulation of potassium ion channels. Pharmacol. Rev. *50*, 723–760.

Yang, Y.Y., Yin, G.L., and Darnell, R.B. (1998). The neuronal RNA-binding protein Nova-2 is implicated as the autoantigen targeted in POMA patients with dementia. Proc. Natl. Acad. Sci. USA *95*, 13254–13259.